# The evolution of the global stellar mass function of star clusters: an analytic description

Lamers, H.J.G.L.M.; Baumgardt, H.; Gieles, M.

[Link to publication](Link to publication)

# The evolution of the global stellar mass function of star clusters: an analytic description

Henny J. G. L. M. Lamers,[1]⋆ Holger Baumgardt[2] and Mark Gieles[3]

[1]*Astronomical Institute Anton Pannekoek, University of Amsterdam, PO Box 94249, NL-1090GE Amsterdam, the Netherlands*
[2]*School of Mathematics and Physics, University of Queensland, QLD 4702 Brisbane, Australia*
[3]*Department of Physics, University of Surrey, Guildford GU2 7XH, UK*

## ABSTRACT

The evolution of the global stellar mass function of star clusters is studied based on a large set of *N*-body simulations of clusters with a range of initial masses, initial concentrations, in circular or elliptical orbits in different tidal environments. Models with and without initial mass segregation are included. The depletion of low-mass stars in initially Roche-volume (tidal) filling clusters starts typically on a time-scale of the order of the core collapse time. In clusters that are initially underfilling their Roche-volume it takes longer because the clusters have to expand to their tidal radii before dynamical mass-loss becomes important.

We introduce the concept of the differential mass function (DMF), which describes the changes with respect to the initial mass function (IMF). We show that the evolution of the DMF can be described by a set of very simple analytic expressions that are valid for a wide range of initial cluster parameters and for different IMFs. The agreement between this description and the models is very good, except for initially Roche-volume underfilling clusters that are severely mass segregated.

**Key words:** stars: luminosity function, mass function – globular clusters: general – open clusters and associations: general – galaxies: star clusters: general.

## 1 INTRODUCTION

The stellar mass function (MF) of the luminous (i.e. non-degenerate) stars of a star cluster changes during the lifetime. This is due to stellar evolution, which turns massive stars into remnants, and due to the stripping of clusters by two-body relaxation in a tidal field and shocks which results in the preferential loss of the lowest mass stars, as was suggested by King (1958). The MF of a cluster depends on its initial mass function (IMF) and on its dynamical evolution. Therefore, the study of the observed MFs of clusters provides information on the IMF and the evolutionary history. For such a study to be successful, we have to understand how the MF of a cluster changes due to dynamical effects. This is the goal of this study.

The theory of preferential mass-loss was pioneered by Hénon (1969) who described the changing MFs of clusters in isolation, from which stars are lost by single, close encounters in the core. Subsequent theoretical and numerical studies of this effect were made by Chernoff & Weinberg (1990), Vesperini (1997), Takahashi & Portegies Zwart (2000), Portegies Zwart et al. (2001), Baumgardt & Makino (2003), Vesperini, McMillan & Portegies Zwart (2009) including the effects of initial mass segregation. Kruijssen (2009)

has expanded the theory of Hénon (1969), by taking into account the tidal field and stellar evolution, mass segregation due to internal relaxation and tidal stripping, including the ejection of stellar remnants. He showed that at any time the escape rate is highest for stars that have a mass of about 1/5 of the most massive stars at that time. This results in a gradual flattening and eventually in a turnover of the MF at the low-mass end.

The purpose of this paper is to derive simple expressions for the predicted evolution of the MF of luminous stars of dissolving star clusters. The expressions are derived from *N*-body simulations of clusters with different masses, half-mass radii, density distributions and in different circular and elliptical orbits. Stellar evolution and dissolution due to tidal stripping and bulge shocks are taken into account. We will show that

(a) the changes in the MF depend mainly on the fraction of the initial mass that is lost and

(b) that these changes can be described by a very simple set of expressions with parameters that depend on the initial conditions and on the mass-loss history.

The expressions can be used to explain observed MFs in terms of initial conditions and/or mass-loss history and to calculate the predicted photometric evolution of star clusters with stellar evolution and dynamical evolution taken into account.

⋆ E-mail: h.j.g.l.m.lamers@uu.nl

The paper is arranged as follows.

In Section 2, we introduce the *N*-body simulations of clusters that form the basis for this study. In Section 3, we describe the expected changes in the MF due to stellar evolution and dissolution. In Section 4, we discuss the evolution of the MF as derived from the *N*-body simulations and introduce the concept of the differential mass function (DMF) . In Section 5, we propose a simple method to describe the evolution of the MF, that agrees well with the models. Section 6 deals with the influence of initial mass segregation on the predicted slope of the MF. The discussion is in Section 7 and the summary is in Section 8. Two appendices describe respectively: a simple way to predict the mass history of a cluster that loses mass by stellar evolution and dissolution and a description of the contribution of stellar remnants to the total mass.

## 2 THE MODELS USED

We use two sets of models, based on *N*-body simulations of initially Roche-volume filling clusters with various orbital parameters by Baumgardt & Makino (2003) (hereafter called BM03) and of initially underfilling (UF) clusters, presented in Lamers, Baumgardt & Gieles (2010) (hereafter called LBG10).

We have selected 25 representative cluster models from BM03, with 8k to 128k stars, with masses $4500 < M < 72\,000\,\mathrm{M}_\odot$, in Galactic orbits of $R_{\mathrm{gal}} = 2.83, 8.5$ and $15\,\mathrm{kpc}$, and with initial density profiles according to King (1966) models with $W_0 = 5$ or 7. For clusters with $M = 18\,000\,\mathrm{M}_\odot$ at $R_{\mathrm{gal}} = 8.5\,\mathrm{kpc}$, we include models in eccentric orbits with $0 \le e \le 0.8$. The clusters have a Kroupa (2001) initial stellar mass function (IMF) in the range of $0.10$–$15\,\mathrm{M}_\odot$, with

$$\mathrm{d}N_i(m)/\mathrm{d}m \propto m^{-2.3} \quad \text{for} \quad m > 0.5\mathrm{M}_\odot$$
$$\propto m^{-1.3} \quad \text{for} \quad m < 0.5\mathrm{M}_\odot. \qquad (1)$$

These models span a range of lifetimes between 2.8 and 46 Gyr. These models and their parameters are listed in the upper half of Table 1.

In order to understand how the changing MF depends on the adopted initial radius of the clusters, the models of BM03 were supplemented with those of initially more compact Roche-volume UF models (LBG2010). The parameters of these 16 models are listed in the lower half of Table 1. They are for clusters with 16k to 128k stars, $10\,000 < M < 72\,000\,\mathrm{M}_\odot$, in circular orbits at $R_{\mathrm{gal}} = 8.5\,\mathrm{kpc}$ with an initial density distribution given by a King profile of $W_0 = 5$, but with initial half-mass radii between 0.5 and 4 pc. This corresponds to tidal-filling factors $\mathfrak{F} \equiv r_{\mathrm{h}}/r_{\mathrm{h}}^{\mathrm{rf}}$ between 0.05 and 0.66, where $r_{\mathrm{h}}$ is the half-mass radius and $r_{\mathrm{h}}^{\mathrm{rf}}$ is the half-mass radius if the cluster were Roche-volume filling. One extra UF model of a cluster orbiting at $R_{\mathrm{gal}} = 2.0\,\mathrm{kpc}$ was added to find the dependence of the evolution of the MF on cluster orbit. The UF models have a Kroupa IMF in the range of $0.1$–$100\,\mathrm{M}_\odot$. In these models 10 per cent of the formed neutron stars and black holes are retained in the cluster.[1] To check the dependence of the results on the adopted IMF, the evolution of a few Roche-volume filling clusters with a Salpeter IMF were also calculated. They will be discussed in Section 5.

To investigate the effect of initial mass segregation, we added two models of clusters with 64k stars in a circular orbit at 8.5 kpc from the Galactic centre. Their initial half-mass radii are 1.0 and 4.0 pc. The Kroupa IMF and their remnant retention factor is the same as used for the UF models. These models, referred to as ufseg1 and ufseg2, are identical to models uf10 and uf12, respectively, apart from their initial mass segregation. The way in which the initial mass segregation was set up has been described in the appendix of Baumgardt, De Marchi & Kroupa (2008). The models are listed in Table 1.

## 3 EXPECTED EVOLUTION OF THE STELLAR MASS FUNCTION

The MF of dissolving clusters changes due to two effects: stellar evolution and dissolution. Stellar evolution removes stars from the high-mass side of the MF, so the upper mass limit of the stars in a cluster decreases with time. Dissolution removes stars of all masses from the cluster.

Due to dynamical friction the massive stars lose total (i.e. potential plus kinetic) energy and sink to the centre of the cluster where they move at high velocity, whereas the low-mass stars gain total energy and move to the outskirts of the cluster where they move at low velocity. This dynamical mass segregation is established on a time-scale

$$t_{\mathrm{seg}}(m) = C(m) \times t_{\mathrm{rh}}, \qquad (2)$$

e.g. Binney & Tremaine (1987), where $t_{\mathrm{rh}}$ is the half-mass relaxation time and $C(m) = A \times <m>/m$ which depends on the MF. The wider the MF, the smaller the value of $A$ (Portegies Zwart & McMillan 2002; Gürkan, Freitag & Rasio 2004; Portegies Zwart, McMillan & Gieles 2010).

There is observational evidence that (some) massive clusters may have *initial* mass segregation due to the star formation process (see reviews by de Grijs & Parmentier 2007; Portegies Zwart et al. 2010).

Before mass segregation is established, the fraction of the stars lost by dissolution is almost independent of the stellar mass. This results in a lowering of the overall normalization of the MF by a time-dependent factor, but preserves the slope of the MF. When the cluster is mass segregated it will preferentially lose low-mass stars from its outskirts. This results in a gradual change in the slope of the MF at the low-mass end. As these changes in the slope are due to dynamical effects, we may expect that they will depend on the mass fraction that is lost by dissolution. (The fraction of luminous mass lost by stellar evolution during the first few Gyrs is about the same, ~45 per cent, for all models).

These considerations imply that the changes in the MF of clusters depend on three time-scales:

(1) the mass-dependent stellar evolution time-scale, $t_{\mathrm{se}}$,
(2) the time-scale for attaining mass segregation, $t_{\mathrm{seg}}$,
(3) the dissolution time-scale, $t_{\mathrm{dis}}$.

If the $t_{\mathrm{seg}} \ll t_{\mathrm{dis}}$, i.e. early mass segregation, then the phase of the gradual lowering of the MF will not occur and the MF will immediately start to flatten at the low-mass end. If $t_{\mathrm{dis}} > t_{\mathrm{se}}$, the MF at the high-mass end will be severely truncated by stellar evolution. Stellar evolution and evaporation after $t_{\mathrm{seg}}$ will both result in an MF that gets narrower with time. Just before complete dissolution the MF of the non-degenerate stars is a narrow peak centred at

---

[1] The difference between the upper limits of 15 and $100\,\mathrm{M}_\odot$ of the two sets of model hardly affects the MF because only 13 per cent of the initial cluster mass is in the range of $15 < m < 100\,\mathrm{M}_\odot$ and the lifetime of these stars is less than 15 Myr. So they have disappeared (apart from a small fraction of their remnants) when dissolution becomes important.

**Table 1.** The $N$-body models used in this study. $R_{gal}$ is the apogalactic distance, $r_J$ is the initial tidal (Jacobi) radius, $r_h$ is the initial half-mass radius, $t_{rh}0$ is the initial half-mass relaxation time and $t_{1\%}$ is the lifetime when the cluster mass is $0.01M_i$. The parameters $\gamma$ and $t_0$ describe the dissolution (see Appendix A) and were derived by LBG10, while $t_{depl}$, $\Delta_{depl}$ and $m_{depl}$ describe the changes in the MF (see Section 5).

| Number | Mass ($M_\odot$) | Number of stars | $W_0$ | $R_{gal}$ (kpc) | Orbit | $r_J$ (pc) | $r_h$ (pc) | $t_{rh}0$ (Gyr) | $t_{1\%}$ (Gyr) | $\gamma$ | $t_0$ (Myr) | $t_{depl}$ (Gyr) | $\Delta_{depl}$ | $\log(m_{depl})$ ($M_\odot$) |
|---|---|---|---|---|---|---|---|---|---|---|---|---|---|---|
| (1) | (2) | (3) | (4) | (5) | (6) | (7) | (8) | (9) | (10) | (11) | (12) | (13) | (14) | (15) |
| 1 | 71952 | 128k | 5 | 15 | circ | 89.6 | 16.75 | 7.20 | 45.3 | 0.65 | 40.0 | 7.41 | −0.21 | 0.05 |
| 2 | 35915 | 64k | 5 | 15 | circ | 71.0 | 13.28 | 3.88 | 26.9 | 0.65 | 42.0 | 5.62 | −0.19 | 0.10 |
| 3 | 18205 | 32k | 5 | 15 | circ | 56.7 | 10.59 | 2.13 | 19.8 | 0.65 | 41.2 | 2.98 | −0.14 | 0.10 |
| 4 | 8808 | 16k | 5 | 15 | circ | 44.5 | 8.32 | 1.13 | 13.4 | 0.65 | 37.9 | 1.60 | −0.09 | 0.08 |
| 5 | 4489 | 8k | 5 | 15 | circ | 35.5 | 6.64 | 0.63 | 9.0 | 0.65 | 36.0 | 1.39 | −0.12 | 0.13 |
| 6 | 71236 | 128k | 5 | 8.5 | circ | 61.1 | 11.43 | 4.05 | 26.5 | 0.65 | 21.5 | 4.40 | −0.18 | 0.08 |
| 7 | 36334 | 64k | 5 | 8.5 | circ | 48.8 | 9.13 | 2.22 | 17.2 | 0.65 | 22.0 | 3.07 | −0.18 | 0.08 |
| 8 | 18408 | 32k | 5 | 8.5 | circ | 39.0 | 7.28 | 1.22 | 11.1 | 0.65 | 21.7 | 1.70 | −0.14 | 0.08 |
| 9 | 9003 | 16k | 5 | 8.5 | circ | 30.7 | 5.74 | 0.65 | 7.5 | 0.65 | 20.5 | 1.54 | −0.16 | 0.15 |
| 10 | 4497 | 8k | 5 | 8.5 | circ | 24.3 | 4.55 | 0.36 | 4.9 | 0.65 | 20.0 | 0.60 | −0.08 | 0.17 |
| 11 | 71218 | 128k | 5 | 2.8 | circ | 29.4 | 5.50 | 1.35 | 9.3 | 0.65 | 7.5 | 1.61 | −0.16 | 0.08 |
| 12 | 35863 | 64k | 5 | 2.8 | circ | 23.4 | 4.37 | 0.73 | 5.9 | 0.65 | 6.7 | 1.11 | −0.15 | 0.12 |
| 13 | 18274 | 32k | 5 | 2.8 | circ | 18.7 | 3.49 | 0.40 | 3.6 | 0.65 | 6.0 | 0.61 | −0.12 | 0.18 |
| 14 | 9024 | 16k | 5 | 2.8 | circ | 14.8 | 2.76 | 0.22 | 2.3 | 0.65 | 5.3 | 0.42 | −0.12 | 0.21 |
| 15 | 4442 | 8k | 5 | 2.8 | circ | 11.7 | 2.18 | 0.12 | 1.3 | 0.65 | 4.4 | 0.22 | −0.09 | 0.31 |
| 16 | 71699 | 128k | 7 | 8.5 | circ | 61.3 | 7.11 | 1.99 | 28.5 | 0.80 | 6.4 | 4.12 | −0.14 | 0.04 |
| 17 | 35611 | 64k | 7 | 8.5 | circ | 48.5 | 5.63 | 1.07 | 17.2 | 0.80 | 6.5 | 2.93 | −0.14 | 0.08 |
| 18 | 18013 | 32k | 7 | 8.5 | circ | 38.7 | 4.48 | 0.58 | 11.2 | 0.80 | 6.5 | 1.58 | −0.11 | 0.09 |
| 19 | 8928 | 16k | 7 | 8.5 | circ | 30.6 | 3.55 | 0.32 | 6.9 | 0.80 | 6.0 | 0.80 | −0.08 | 0.14 |
| 20 | 4402 | 8k | 7 | 8.5 | circ | 24.2 | 2.80 | 0.17 | 4.4 | 0.80 | 5.5 | 0.50 | −0.07 | 0.18 |
| 21 | 17981 | 32k | 5 | 8.5 | e0.2 | 29.5 | 5.51 | 0.80 | 9.0 | 0.65 | 14.5 | 1.80 | −0.15 | 0.12 |
| 22 | 18300 | 32k | 5 | 8.5 | e0.3 | 25.7 | 4.81 | 0.65 | 7.8 | 0.65 | 12.0 | 1.14 | −0.09 | 0.16 |
| 23 | 17966 | 32k | 5 | 8.5 | e0.5 | 18.6 | 3.47 | 0.40 | 5.7 | 0.65 | 8.8 | 0.80 | −0.07 | 0.18 |
| 24 | 17957 | 32k | 5 | 8.5 | e0.7 | 12.2 | 2.27 | 0.21 | 3.6 | 0.65 | 5.9 | 0.58 | −0.08 | 0.22 |
| 25 | 18026 | 32k | 5 | 8.5 | e0.8 | 8.9 | 1.67 | 0.13 | 2.8 | 0.65 | 4.5 | 0.35 | −0.03 | 0.25 |
| uf1 | 10405 | 16k | 5 | 8.5 | circ | 32.2 | 0.50 | 0.02 | 6.08 | 0.80 | 5.5 | 0.68 | −0.08 | 0.15 |
| uf2 | 10831 | 16k | 5 | 8.5 | circ | 32.6 | 1.00 | 0.05 | 7.22 | 0.80 | 5.1 | 0.83 | −0.05 | 0.13 |
| uf3 | 10426 | 16k | 5 | 8.5 | circ | 32.2 | 2.00 | 0.13 | 7.59 | 0.80 | 6.2 | 1.00 | −0.04 | 0.11 |
| uf4 | 10589 | 16k | 5 | 8.5 | circ | 32.4 | 4.00 | 0.36 | 5.89 | 0.80 | 5.0 | 1.07 | −0.08 | 0.11 |
| uf5 | 21059 | 32k | 5 | 8.5 | circ | 40.7 | 0.50 | 0.02 | 9.55 | 0.80 | 5.5 | 0.77 | −0.05 | 0.14 |
| uf6 | 21193 | 32k | 5 | 8.5 | circ | 40.8 | 1.00 | 0.06 | 11.42 | 0.80 | 5.0 | 1.37 | −0.05 | 0.11 |
| uf7 | 21095 | 32k | 5 | 8.5 | circ | 40.7 | 2.00 | 0.17 | 13.40 | 0.80 | 6.0 | 1.60 | −0.04 | 0.08 |
| uf8 | 20973 | 32k | 5 | 8.5 | circ | 40.7 | 4.00 | 0.47 | 12.75 | 0.80 | 6.0 | 1.94 | −0.08 | 0.08 |
| uf9 | 41980 | 64k | 5 | 8.5 | circ | 51.2 | 0.50 | 0.03 | 15.20 | 0.80 | 5.5 | 1.25 | −0.06 | 0.10 |
| uf10 | 41465 | 64k | 5 | 8.5 | circ | 51.0 | 1.00 | 0.08 | 17.79 | 0.80 | 5.0 | 1.67 | −0.03 | 0.07 |
| uf11 | 40816 | 64k | 5 | 8.5 | circ | 50.8 | 2.00 | 0.21 | 20.76 | 0.80 | 6.5 | 2.81 | −0.04 | 0.06 |
| uf12 | 42114 | 64k | 5 | 8.5 | circ | 51.3 | 4.00 | 0.61 | 21.18 | 0.80 | 6.0 | 3.10 | −0.06 | 0.05 |
| uf13 | 83439 | 128k | 5 | 8.5 | circ | 60.4 | 1.00 | 0.10 | 30.03 | 0.80 | 7.2 | 3.01 | −0.04 | 0.05 |
| uf14 | 83853 | 128k | 5 | 8.5 | circ | 64.5 | 2.00 | 0.28 | 34.77 | 0.80 | 7.0 | 4.43 | −0.03 | 0.04 |
| uf15 | 83700 | 128k | 5 | 8.5 | circ | 64.5 | 4.00 | 0.80 | 36.58 | 0.80 | 7.2 | 5.12 | −0.04 | 0.04 |
| uf16 | 41465 | 64k | 5 | 2.0 | circ | 19.4 | 1.00 | 0.08 | 7.14 | 0.80 | 1.2 | 0.98 | −0.04 | 0.12 |
| ufseg1 | 41465 | 64k | 5 | 8.5 | circ | 51.0 | 1.00 | 0.07 | 18.48 | 0.80 | 6.0 | 1.86 | 0.00 | 0.07 |
| ufseg2 | 42113 | 64k | 5 | 8.5 | circ | 51.3 | 4.00 | 0.60 | 9.90 | 0.80 | 4.0 | 0.48 | 0.00 | 0.10: |

a mass that corresponds roughly to the turnoff mass of the main sequence.

## 4 RESULTS OF *N*-BODY SIMULATIONS

### 4.1 The dependence of the MF on $\mu = M(t)/M_i$

The top panel of Fig. 1 shows the MFs of two models that have almost the same total dissolution time, $t_{1\%}$, at fixed values of $\tau = t/t_{1\%} = 0$, 0.5, 0.8 and 0.9. The MFs of the models are significantly different, especially at later times. This shows that the dynamical age, $\tau \equiv t/t_{1\%}$, is not a good parameter to describe the changes in the MF for low-mass stars. The lower panel of Fig. 1

shows the MF of the same models as in the left-hand panels, but now the MFs at the same values of the remaining mass fractions $\mu = M(t)/M_i$ are compared.[2]

We see that the MFs of different models agree much better with one another if they are compared at the same value of $\mu$. The same result was found by Trenti, Vesperini & Pasquato (2010) based on a different set of cluster models.

The fact that the shape of the MF depends on $\mu$ and not on $\tau$ shows that stars are lost in a preferred order, depending on their

---

[2] The mass fraction $\mu = M/M_i$ includes the contributions by remnants. The mass fraction $\mu_{lum} = M_{lum}/M_i$ is for luminous (non-degenerate) stars only.
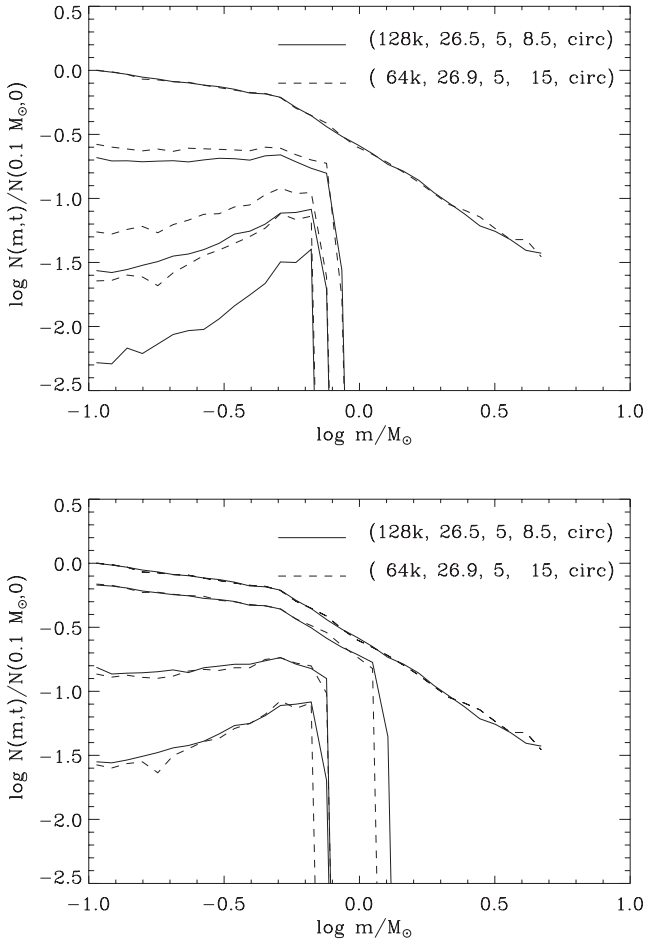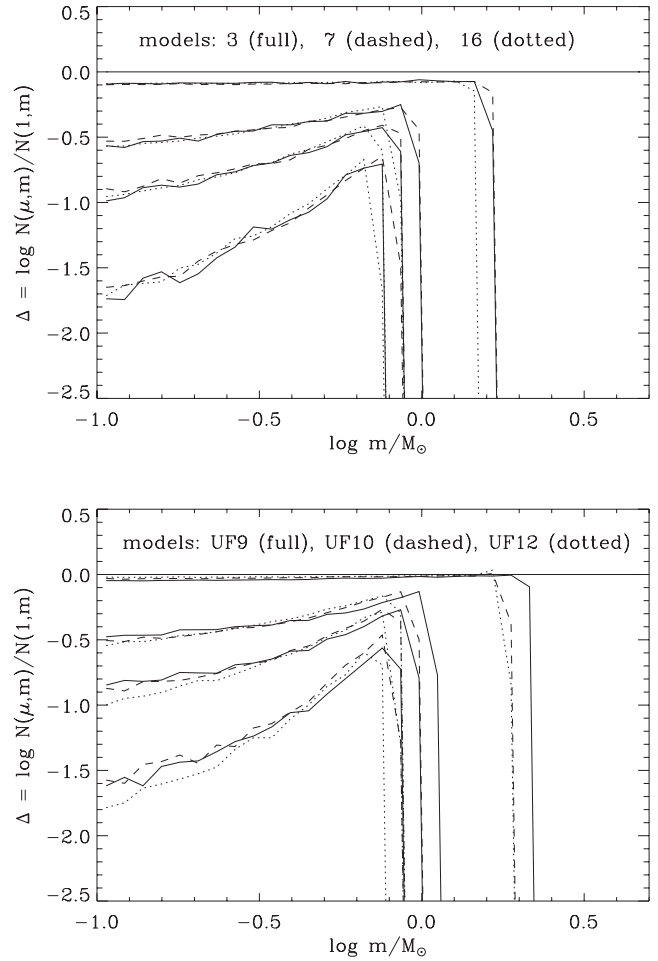
**Figure 1.** Comparison between the MFs in logarithmic bins of $\Delta \log m = 0.0567$ of a pair of BM03 cluster models (number 6, full lines and number 2, dashed lines) with similar dissolution times. The MF is normalized to the value at $0.1\,\mathrm{M}_\odot$ at $t = 0$. The models are specified by a vector which gives (number of stars, $t_{1\%}$(Gyr), $W_0$, orbit in $R_G$ and eccentricity). Top: the MFs at different times: $\tau = t/t_{1\%} = 0$ (upper curves), 0.5, 0.8 and 0.9 (lowest curves). Bottom: the MFs of the same pair of models at different residual mass fractions: $\mu = M(t)/M_i = 1.0$ (upper curves), 0.5, 0.2 and 0.1 (lowest curves). In this representation the MFs of the pair of models are very similar.



**Figure 2.** Top: the DMFs expressed in $\Delta(\mu, m)$ of three models (numbers 3, 7 and 16) of initially Roche-volume filling clusters with very different numbers of stars, orbits and ages. The DMFs are shown for $\mu = 1.0$ (horizontal line), 0.60, 0.30, 0.20 and 0.10. Bottom: the DMFs of three models (numbers uf9, uf10 and uf12) with different initial half-mass radii of 0.5, 1 and 4 pc at the same values of $\mu$ as in the top figure. Although the characteristics of the models are very different the DMFs at the low-mass end are quite similar. At the high-mass end the MFs are truncated by stellar evolution.

mass and independent of the speed with which this happens. After mass segregation has been established by two-body relaxation the low-mass stars are in the outer shells and are lost preferentially. Since most of the cluster mass is in the low-mass stars, a significant change in $\alpha$ will automatically imply a reduction of $\mu$. (In this simple explanation we have ignored the mass-loss by stellar evolution.) These arguments show that we can expect that the MF of clusters in different orbits, different initial masses and different dissolution times will be approximately the same if they are compared at the same value of $\mu$.[3]

### 4.2 The differential mass function

We express the changes in the MF in terms of the logarithm of the fraction of stars lost as function of the stellar mass,

---

[3] Kruijssen (2009) has shown that the MF of clusters also depends on the retention factor of stellar remnants.

$\Delta(t, m) \equiv \log(N(t, m)/N(t = 0, m))$, where $N(t, m)$ is the number of stars per linear mass interval at time $t$. Based on the arguments presented in Section 4.1, we describe $\Delta$ as a function of $\mu$ instead of $t$. So we can write

$$\Delta(\mu, m) \equiv \log N(\mu, m)/N(1, m), \qquad (3)$$

where $N(1, m) \equiv N_i(m)$ is the IMF. We will call this the differential mass function (DMF).

Fig. 2 shows the DMF for a characteristic subset of three initially Roche-volume filling models (upper panel) and three Roche-volume UF models with $r_{h0} = 0.5$, 1 and 4 pc (lower panel) which have different mass-loss histories. Although the three clusters in each panel have different characteristics the DMF at the low-mass end of all models are similar. The DMF at the high-mass end is strongly variable due to stellar evolution, with the mass truncation being most severe for clusters with long dissolution times. The figure shows that for large values of $\mu \gtrsim 0.60$ the DMF is horizontal because the cluster is not yet mass segregated and stars of all masses have about equal probability of being lost. This implies that in these
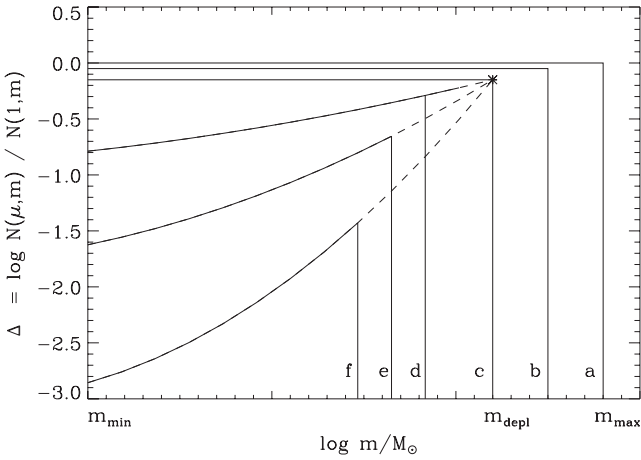
**Figure 3.** A schematic description of the DMF, $\Delta(\mu, m)$ with $\mu = M/M_i$. The upper mass limit decreases due to stellar evolution. Before mass segregation (lines a,b,c) $\Delta$ decreases independent of the stellar mass $m$. After mass segregation (lines d,e,f) the shape of $\Delta$ is described by a simple steepening function of mass around a 'depletion point', indicated by an asterisk.

models the preferential loss of low-mass stars does not set in before $\mu \simeq 0.6$. At that time about 30 per cent of the mass is lost by stellar evolution and about 10 per cent by dissolution. This is because the models do not have initial mass segregation and it takes several half-mass relaxation times to establish mass segregation as will be shown below. Later, when $\mu \lesssim 0.60$, the slope of the DMF steepens with decreasing $\mu$.

The shapes of the DMFs of *all* models, including those not shown here, are very similar. This result is the basis for a simple description of the MF evolution of all cluster models.

# 5 AN ANALYTIC DESCRIPTION OF THE CHANGING MF

Because the DMFs of all models are very similar, we can derive a simple description that allows the calculation of the MFs of the luminous stars (non-remnants). The method is schematically shown in Fig. 3 which can be compared with the observed DMFs of Fig. 2. It has the following characteristics.

At young ages, before low-mass depletion has set in, i.e. at $\mu > \mu_{\mathrm{depl}}$, the value of $\Delta(\mu, m)$ decreases independent of $m$. At the same time stellar evolution removes the most massive stars. This behaviour continues until the cluster is mass segregated and dynamical effects start to deplete the clusters of low-mass stars. Then DMF turns down at the low-mass side, with a slope that gets steeper and a curvature that gets stronger as time progresses and the luminous mass decreases. The point where the DMF starts to turn down is called the 'depletion point' in the $\Delta$ versus $\log(m)$ diagram, with coordinates $\log(m_{\mathrm{depl}})$ and $\Delta_{\mathrm{depl}}$.

At any time during the evolution of the cluster the MF of luminous stars is described by $N(m) = N_i(m).10^{\Delta(\mu, m)}$ (equation 3). The total luminous mass is

$$M_{\mathrm{lum}} \equiv \mu_{\mathrm{lum}} M_i = \int_{m_{\mathrm{min}}}^{m_{\mathrm{max}}(t)} N_i(m).m.10^{\Delta(\mu, m)} \mathrm{d}m, \qquad (4)$$

where $m_{\mathrm{min}}$ is the minimum stellar mass and $m_{\mathrm{max}}(t)$ is the maximum stellar mass left after evolution at cluster age $t$ when the cluster mass is $M(t) = \mu M_i$.

## 5.1 Changes in the MF before mass segregation: $t < t_{\mathrm{depl}}$ and $\mu > \mu_{\mathrm{depl}}$

Before mass segregation the value of $\Delta(\mu, m)$ decreases independent of $m$. In case of no dissolution $\mu_{\mathrm{lum}}(t) = \mu_{\mathrm{lum}}^{\mathrm{se}}(t)$ which is the integral of $N_i(m) \times m$ between $m_{\mathrm{min}}$ and $m_{\mathrm{max}}(t)$. With dissolution $N(\mu, m) = 10^{-\Delta(\mu, m)} N_i(m)$ and so

$$\Delta(\mu, m) = \log(\mu_{\mathrm{lum}}/\mu_{\mathrm{lum}}^{\mathrm{se}}(t)) \qquad (5)$$

at $\mu > \mu_{\mathrm{depl}}$, where $\mu_{\mathrm{lum}} = M_{\mathrm{lum}}/M_i$ is the fraction of the luminous mass. The value of $1 - \mu_{\mathrm{lum}}^{\mathrm{se}}(t)$ is the fraction of the initial mass that is lost by stellar evolution at time $t$. It can easily be calculated from the power-law approximations in appendix B of LBG2010 for different metallicities.

## 5.2 The shape of the DMF at $t > t_{\mathrm{depl}}$ and $\mu < \mu_{\mathrm{depl}}$

The cluster models show that the changes in the DMF can be described by slightly curved lines that get steeper and more curved as the remaining mass fraction decreases. (For instance see Fig. 2). A study of *all* N-body models of Table 1 shows that at $\mu < \mu_{\mathrm{depl}}$ the slope of the DMF can be expressed accurately by a second-order polynomial of $\log(m/m_{\mathrm{depl}})$,

$$\Delta(\mu, m) = a_0 + a_1 \times l + a_2 \times l^2 \qquad (6)$$

with $l \equiv \log(m/m_{\mathrm{depl}})$, $a_0 = \Delta_{\mathrm{depl}}$, $a_1$ is a time-dependent parameter and $a_2 = 0.356 a_1 + 0.019 a_1^2$. The second-order polynomial relation between $a_2$ and $a_1$ is also derived from the MF of the models.
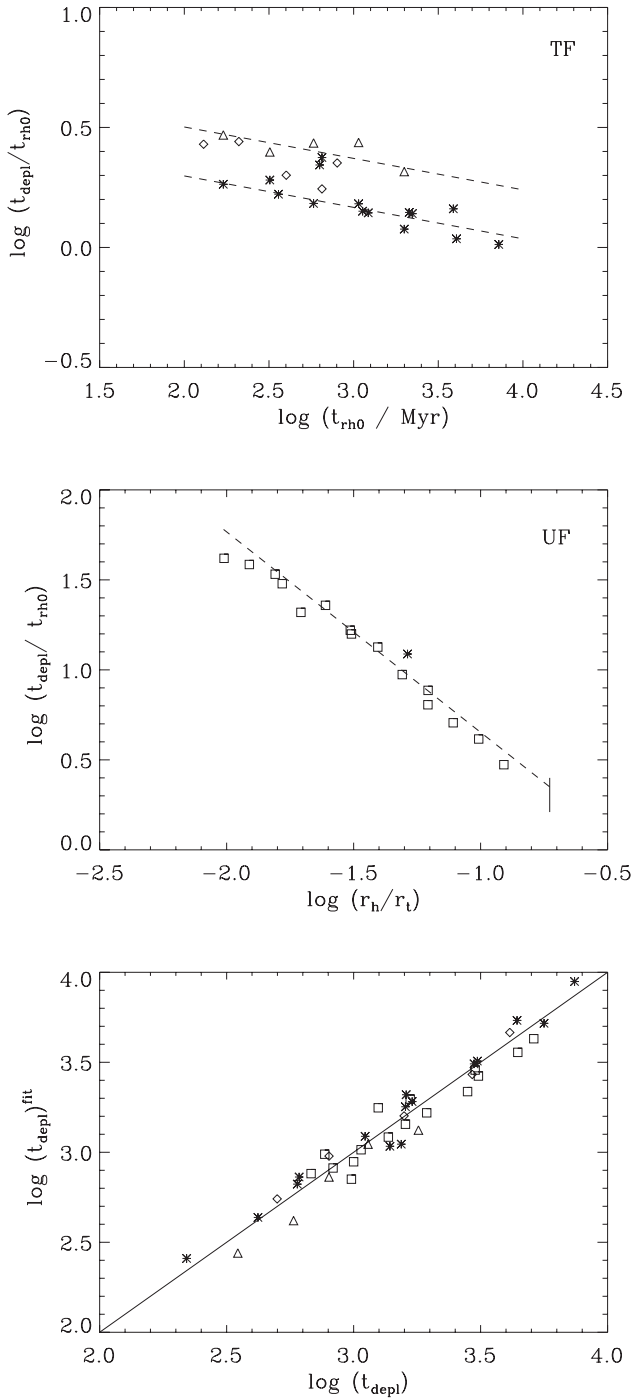
This function goes through the depletion point, where the DMF starts to curve down for low-mass stars, because $l = 0$ at $m = m_{\mathrm{depl}}$ and so $\Delta(\mu, m_{\mathrm{depl}}) = \Delta_{\mathrm{depl}}$ for all values of $\mu$ and has the property that the second derivative $a_2$ is a function of the first derivative $a_1$, i.e. the curvature gets stronger as $\mu$ decreases and more low-mass stars are lost (see Figs 2 and 3).

The value of $a_1$, and by consequence also of $a_2$, depends on $\mu$ because it describes the steepness of the DMF at $m < m_{\mathrm{depl}}$. The numerical value of $a_1$ is set by the condition that equation (4) for $M_{\mathrm{lum}}(\mu)$ is satisfied. So there is direct coupling between $a_1$ and $M_{\mathrm{lum}}/M_i$.

The curvature of $\Delta$ has been explained by Kruijssen (2009), who showed that the preferential loss of low-mass stars is due to two competing effects: (a) a low-mass star can most easily gain energy by encounters with stars of much higher mass, but (b) when the cluster is mass segregated the most massive stars are deep inside the cluster so the probability of encounters with very massive stars is small. Kruijssen has shown that for a Kroupa IMF the largest escape rates occur for stars with $m \sim 0.2 m_{\mathrm{max}}$, where $m_{\mathrm{max}}$ is the mass of the most massive star at that time (see his fig. 4). So the removal rate of the lowest mass stars is less than expected from a linear extrapolation of the DMF from $m_{\mathrm{depl}}$ to $m_{\mathrm{min}}$.

## 5.3 The depletion point: $m_{\mathrm{depl}}$ and $\Delta_{\mathrm{depl}}$

We have derived the values of $m_{\mathrm{depl}}$ for all models by fitting second-order polynomials of $\Delta(\mu, m)$ versus $\log(m)$ for each model at $\mu = 0.6, 0.5, 0.3, 0.2$ and $0.1$ and deriving the value of $\log(m)$ where these curves cross each other. We found that for each model these polynomials for the different values of $\mu$ all cross at about the same value of $\log(m)$ with a very small scatter. The mean value of these crossing points was then adopted to be $\log(m_{\mathrm{depl}})$ for that model. The resulting values of $\log m_{\mathrm{depl}}$ and $\Delta_{\mathrm{depl}}$ are listed in Table 1, columns 15 and 14. The estimated accuracy of $\log(m_{\mathrm{depl}})$ is about

The values of $m_{depl}$ depend on the parameters of the clusters, in particular on the time of mass segregation. Spitzer (1969) has shown that mass segregation for a star of mass $m$ occurs on a time-scale proportional to the half-mass relaxation time (equation 2).

This implies that for clusters without initial mass segregation, changes in the MF will start to be noticeable after a number of elapsed half-mass relaxation time-scales. Clusters with a short $t_{rh}$ will reach mass segregation earlier and will also have a shorter lifetime than clusters with a long $t_{rh}$.

Let us define the depletion time, $t_{depl}$, as the time when the DMF at $m = 0.2 M_{\odot}$ is 0.02 smaller than that at $m = 0.5 M_{\odot}$. This is a well-defined time that can easily be derived from the models. The values of $t_{depl}$ are listed in Table 1, column 13. Fig. 4 shows the dependence of $t_{depl}$ on $t_{rh0}$ for initially tidal-filling models (numbers 1 to 25) in the top panel, whereas the middle panel shows the nearly linear relation between $t_{depl}/t_{rh0}$ and $r_{h0}/r_J$ for the initially UF models (numbers uf1 to uf16). We found that for all models without initial mass segregation used here, i.e. initially Roche-volume filling and UF, the depletion of low-mass starts at about at an age
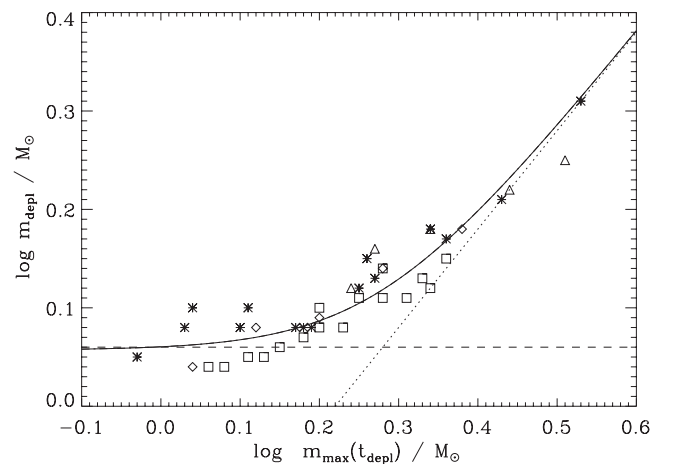
$$\log(t_{depl}) \simeq -0.210 + 0.873 \times \log(t_{rh0}) - 1.084 \times \log(r_{h0}/r_J)_i, \quad (7)$$

with $t_{depl}$ and $t_{rh0}$ in units of Myrs (see Fig. 4). The almost linear dependence of $t_{depl}$ on $t_{rh0}$ agrees with the theory. The dependence of $t_{depl}$ on $r_{h0}/r_J$ is due to the fact that we used the *initial* value of $t_{rh}$. Clusters that start very compact will first expand as they lose mass by stellar evolution. This results in an increase in $t_{rh}$ and since segregation will occur after a number of *elapsed actual* relaxation times, the relation between $t_{depl}$ and $t_{rh0}$ needs a correction that depends on the initial concentration.

The mass of the depletion point $m_{depl}$ is expected to depend on the maximum stellar mass at the time of mass segregation, $m_{max}(t_{depl})$, and the mass of the remnants at that time. We can expect a relation of the type

$$m_{depl} = \max[a \times m_{max}(t_{depl}), m_{rem}] \quad (8)$$

with $a < 1$, and $m_{rem}$ is the mean mass of the remnants that are efficient in ejecting stars when they are more massive than stars at the turnoff point. Fig. 5 shows the relation between $m_{max}(t_{depl})$ and $m_{depl}$ for all our models. This figure shows the expected trend: $m_{depl} \propto m_{max}(t_{depl})$ at large $m_{max}(t_{depl})$ and $m_{depl} \simeq$ constant at small

**Figure 4.** Top: the ratio $t_{depl}/t_{rh0}$ versus $t_{rh0}$ for tidal-filling clusters. Stars: $W_0 = 5$ models in circular orbits, diamonds: $W_0 = 7$ models, triangles: models in eccentric orbits. The two dotted lines are mean relations for $W_0 = 5$ and 7 models. Middle: the ratio $t_{depl}/t_{rh0}$ for UF clusters as a function of the initial ratio $r_h/r_J$. The star is for model uf16 at $R_G = 2.0$ kpc, the squares are for models at $R_G = 8.5$ kpc. The dashed line is the mean relation. The short vertical line shows the range of values for tidal-filling clusters of $W_0 = 5$ with $0.03 < t_{rh0} < 1$ Gyr. Lower: comparison between the value of $t_{depl}$ derived by equation (7) and the values in Table 1.

0.02 to 0.03 dex. The values of $\Delta_{depl}$ (Table 1) range from $-0.21$ to $-0.03$, indicating that the clusters have lost between 7 and 40 per cent of their mass by dissolution before the depletion of low-mass stars sets in.



**Figure 5.** The relation between $m_{max}(t_{depl})$ and $m_{depl}$ for all cluster models. The symbols are the same as in Fig. 4. The two expected asymptotic relations, i.e. $m_{depl} \propto m_{max}(t_{depl})$, and $m_{depl} \simeq$ constant are shown by dashed lines. The full line shows the adopted relation of equation (9).
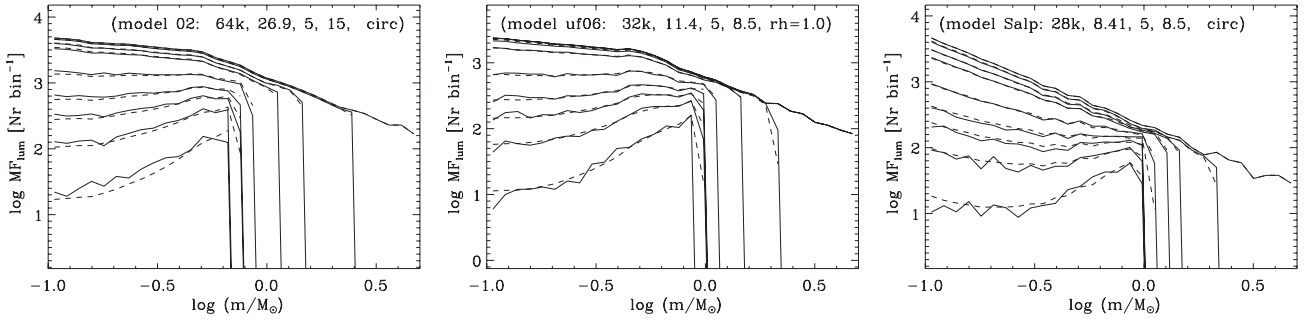
**Figure 6.** Comparison between the MF (full lines), in terms of $\log(N)$ per logarithmic mass bins of 0.0567 dex, of a few characteristic $N$-body models with a Kroupa IMF at nine values of $\mu = 1.0, 0.75, 0.60, 0.50, 0.30, 0.20, 0.15, 0.10$ and $0.05$ (from top to bottom) with the simple description (dashed) of Section 5. The models are indicated in each panel by the same parameters as in Fig. 2. The last model has a Salpeter IMF in the range of $0.1$–$100\,M_\odot$.

$m_{\max}(t_{\rm depl})$ with a transition region in between. We can fit the data to a function that has this asymptotic behaviour:

$$m_{\rm depl} = \left[ (1.14)^x + (0.60 \times m_{\max}(t_{\rm depl}))^x \right]^{1/x} \qquad (9)$$

with $x = 5$ and masses in $M_\odot$.

The fraction of the mass that is lost dynamically before low-mass depletion starts, $\Delta_{\rm depl}$, covers a small range of $-0.03$ for the short-lived models to $-0.21$ for the longest living models. The initially Roche-volume filling clusters lose a considerable fraction of their mass at an early phase by evolution-induced dynamical mass-loss, when the cluster expands due to the fast mass-loss by stellar evolution (LBG10). For these models we can express $\Delta_{\rm depl} \simeq 0.35 - 0.12\,\log(t_{1\%}/{\rm Myr})$ with a scatter of about 0.05. The initially Roche-volume UF clusters do not suffer evolution-induced mass-loss, because at the time of high mass-loss by stellar evolution they do not yet fill their Roche-volume. For these models we find that $\Delta_{\rm depl} \simeq -0.06$, with a scatter of about 0.02. The initially mass segregated models have $\Delta_{\rm depl} = 0$ (see below).

### 5.4 Comparison with *N*-body models

Fig. 6 shows examples of the comparison between the MFs of the models and those predicted by our analytical expressions for a few *N*-body models: an initially tidal-filling model (left) and a severely UF model (middle). We used the values of $m_{\rm depl}$ derived from equations (7) and (9) and $\Delta_{\rm depl}$ from the description above. These models cover a large range of initial conditions such as initial mass, tidal field and total lifetime, from 26.9 to 8.4 Gyr. The agreement is equally good for the models that are not shown here.[4]

To check that our description of the DMF is not only valid for clusters with a Kroupa IMF, we performed *N*-body simulations of a cluster of 28196 stars and an initial mass of $9007.6\,M_\odot$, distributed with a Salpeter (1955) power-law IMF of index $-2.35$ in the mass range of $0.10$–$100\,M_\odot$. The cluster is in a circular orbit at a galactocentric distance of 8.5 kpc. The total lifetime of the cluster is 9.56 Gyr and $t_{1\%} = 8.41$ Gyr. The initial half-mass radius is 5.7 pc and the initial half-mass relaxation time is 1.045 Gyr. 90 per cent of the neutron stars and black holes are kicked at birth, similar to the other UF models. The last panel of Fig. 6 shows the very good agreement between the MF of the model and our simple description in Section 5. This suggests that our analytic description of the

evolution of the DMF may also be applied to clusters with other IMFs, provided that they do not deviate strongly from a Kroupa or Salpeter IMF.

## 6 CLUSTERS WITH INITIAL MASS SEGREGATION

Two of our models, ufseg1 and ufseg2, are initially mass segregated. The set-up of the mass segregation is the same as used by Baumgardt et al. (2008), which corresponds to 100 per cent mass segregation. The properties of these models are listed in the last two lines of Table 1. Apart from the initial mass segregation, the initial properties of these models are the same as those of models uf10 and uf12, respectively. Models ufseg1 and uf10 have an initial half-mass radius of 1 pc whereas models ufseg2 and uf12 have $r_{\rm h} = 4.0$ pc. For understanding the effect of the initial mass segregation we compare the evolution of MFs of these models in pairs.

Fig. 7 shows the DMF of the model pairs at different residual mass fractions. The DMFs of models ufseg1 and uf10 are very similar. For these models the initial mass segregation hardly plays a role: they both reach the same age and although ufseg1 is initially mass segregated, its values of $t_{\rm depl}$, $\Delta_{\rm depl}$ and $\log(m_{\rm depl})$ are very similar to those of uf10.
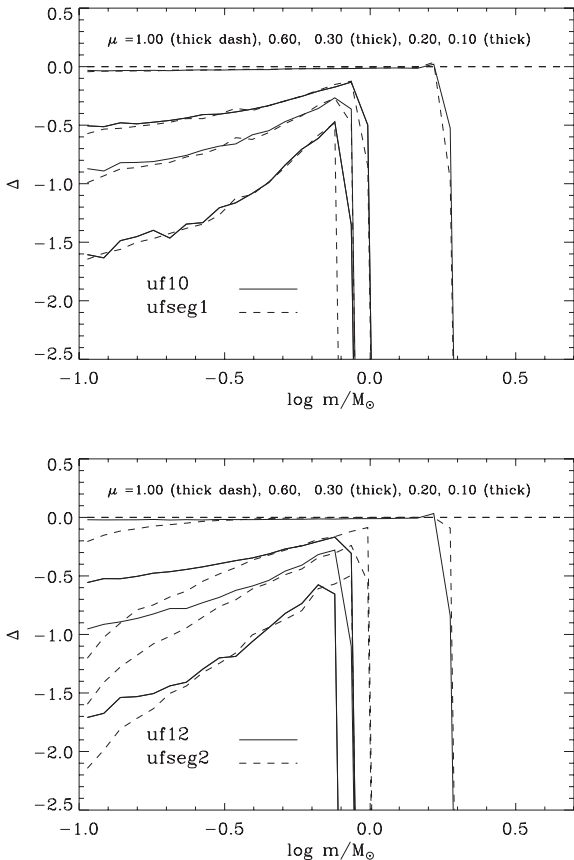
On the other hand, the evolution of models ufseg2 and uf12 are very different: uf12 reaches an age of 21 Gyr, but ufseg2 reaches only 9.9 Gyr. This is also reflected in the difference between $t_0 = 6.0$ Myr for uf12 and 4.0 Myr for ufseg2. So the dynamical mass-loss rate of the ufseg2 is much higher than that of uf12. When the DMF is compared at values of the same $\mu$ for both models, we find that the low-mass end of the MF at $m < 0.5$ is much lower in the initially mass segregated model. It obviously loses more low-mass stars than the one that starts without mass segregation. This is also reflected in a smaller value of $t_{\rm depl}$. As a result, our analytic description of the MF evolution agrees very well with that of model ufseg1, but underestimates the low-mass star depletion of model ufseg2.

What is the reason that the initial mass segregation has a much stronger effect on model ufseg2 with $r_{\rm h} = 4$ pc than on model ufseg1 with $r_{\rm h} = 1$ pc, both in terms of a significantly shorter lifetime and a stronger depletion in the lowest mass stars?

Significant mass-loss will only set in when a cluster has expanded to its tidal limit ($r_{\rm J}$). If that happens *after* the cluster has gone into core contraction, then the presence or absence of initial mass segregation is not important because core contraction results in mass segregation anyway. However, if the cluster reaches its tidal limit due to expansion by stellar mass-loss *before* it goes into core

---

[4] The truncation at the high-mass end is not sharp because the model data and the predicted data are both calculated and plotted at logarithmic mass intervals.

**Figure 7.** Comparison between the evolution of the DMFs of models with and without initial mass segregation. The upper panel compares model ufseg1 (dashed) with uf10 (full); the middle panel compares models ufseg2 (dashed) with uf12 (full). The lines refer to times when $\mu = 1$ (horizontal), 0.6, 0.3, 0.2 and 0.1 (lowest). Notice that initial mass segregation has a much stronger effect on model ufseg2 with $r_{\rm h} = 4.0$ pc than on model ufseg1 with $r_{\rm h} = 1.0$ pc.

**Table 2.** Comparing models with and without initial mass segregation.

| Property | uf10 | ufseg1 | uf12 | ufseg2 |
|---|---|---|---|---|
| Segregated | No | Yes | No | Yes |
| $r_{\rm h0}$ (in pc) | 1.0 | 1.0 | 4.0 | 4.0 |
| $r_{\rm lim}$ (in pc) | 5.3 | 5.3 | 21.4 | 21.4 |
| $r_{\rm J}$ (in pc) | 51.0 | 51.0 | 51.3 | 51.3 |
| $r_{\rm J}/r_{\rm lim}$ | 9.6 | 9.6 | 2.4 | 2.4 |
| $t_{\rm rh0}$ (in Myr) | 70 | 70 | 600 | 600 |
| $t_{\rm exp}(r_{\rm J})$ (in Myr) | 8800 | <8800 | 4300 | ≪4300 |
| $t_{\rm cc}$ (in Myr) | 4400 | 4400 | 13 200 | 13 200 |
| $t_{1\%}$ (in Myr) | 17 900 | 18 500 | 21 200 | 9900 |

collapse, the radial distribution of the MF will still reflect the initial one (Baumgardt et al. 2008). So the key question is: did cluster models ufseg1 and ufseg2 reach their tidal limit before or after they went into core collapse?

Table 2 gives some of the characteristic values of cluster models uf10 and uf12 without and ufseg1 and ufseg2 with initial mass segregation. This table gives the initial half-mass radius $r_{\rm h0}$, the initial radius limit of the clusters $r_{\rm lim} = r_{\rm h}/0.186$ for $W_0 = 5$ models, the tidal radius, $r_{\rm J}$, and the initial ratio $r_{\rm J}/r_{\rm lim}$. This last number is the factor of radius increase before the cluster reaches the tidal limit

and starts losing mass efficiently. Models uf12 and ufseg2 have to expand only by a factor of 2.4 before reaching the tidal limit whereas models uf10 and ufseg1 have to expand by almost a factor of 10. We also give the initial half-mass relaxation time, the expansion time (defined below), the core-collapse time and the total lifetime.

The radius evolution of clusters due to stellar evolution and core collapse has been described by Gieles et al. (2010) for clusters deep within their tidal boundary (isolated clusters). They showed that for models which keep their initial density distribution the radius expands approximately as

$$r_{\rm h} \simeq r_{\rm h0} \cdot \left[ (t/t_*)^{2\delta} + (\chi t/t_{\rm rh0})^{4/3} \right]^{1/2}, \qquad (10)$$

where $\delta = 0.07$, $t_* = 2$ Myr and $\chi \simeq 3(t/t_*)^{-0.3}$. The first term describes the initial adiabatic expansion (i.e. when the mass-loss time-scale is longer than the crossing time) due to mass-loss by stellar evolution and the second term is the following expansion due to the heating by binaries in the core after core collapse. Using this expression, we estimate the time it takes for these cluster models to expand to the Jacobi radius, $t_{\rm exp}(r_{\rm J})$ in Table 2.

The expansion due to evolutionary mass-loss in equation (10) was derived by assuming that the mass-loss occurs from all over the cluster, i.e. without mass segregation. In that case, the radius expands inversely proportional to the remaining mass fraction, which is more than about 0.6 $M_{\rm i}$ in a Hubble time. This limits the expansion due to stellar evolution to about a factor of 1.5. However, when the cluster is initially mass segregated the stellar mass is lost from the centre where the density is highest. This means that the potential energy of the cluster increases much stronger than predicted for unsegregated clusters and so the cluster will expand much more due to evolutionary mass-loss (Vesperini et al. 2009).

Since cluster model ufseg2 needs an expansion factor of only 2.4, it reaches its tidal limit early on during the stellar mass-loss phase and well before core contraction, when the initial extreme mass segregation is still imprinted in the cluster. This explains (a) why the MF drops steeply at very low masses (more than initially mass segregated model ufseg1) and (b) why the lifetime of the cluster is much shorter than that of the model uf12 without initial mass segregation. Here we remind that models ufseg1 and ufseg2 started with extreme mass segregation which is unlikely to happen in real clusters. Therefore, we expect that the low-mass star depletion of real clusters with initial mass segregation will be less severe than predicted by model ufseg2.

## 7 DISCUSSION

We have studied the evolution of the global stellar MF of clusters, based on the results of a large grid of *N*-body simulations. As our formalism is derived from a specific grid of *N*-body simulations, we discuss the influence of these simulations.

(1) *The influence of binaries.* The *N*-body models do include the effect of binaries that are formed in the cluster, but not the effect of initial binaries. As a first approximation we may describe the effect of binaries as that of the presence of more massive stars than in the IMF. Kruijssen (2009) has shown that stars with a mass of about 15 to 20 per cent of the most massive stars have the highest ejection probability. Equal mass binaries would increase the mass of the most massive objects by about factor of 2 or so. The presence of massive objects (black holes or binaries) in a cluster increases the ejection rate of intermediate mass stars ($1–3$ M$_\odot$) compared to those of low-mass stars. This means that the DMF will remain flatter than in the absence of binaries. However, we do not expect this effect to be strong because most massive remnants will be ejected from the

cluster by their kick-velocity (in our models only 10 per cent of the neutron stars and black holes are retained), and the initial presence of a large fraction of nearly equal mass binaries is unlikely.[5]

(2) *The influence of the IMF.* All *N*-body models that we used have a Kroupa IMF and our description of the evolution of the MF is derived for these models. Since we describe the evolution of the MF in terms of a *differential* effect, i.e. MF(t) compared to the IMF, we expect that this DMF is not very sensitive to the shape of the IMF, except if the IMF would differ strongly from a Kroupa IMF. As a test we compared the results of one model with a Salpeter IMF with our prediction based on the DMF concept. We found a very good agreement between prediction and theory (lower panel of Fig. 6). One of the reasons for this agreement is the fact that the Kroupa IMF and the Salpeter IMF only differ at masses below $0.5 M_\odot$, whereas most of the depletion of low-mass stars is the result of encounters with stars of $M > 0.5 M_\odot$. Our analytic description may fail for clusters with a strongly different IMF.

(3) *The effect of initial mass segregation.* The majority of the models discussed above did not have initial mass segregation, although there is indirect evidence in the presence of globular clusters (GCs), (e.g. Baumgardt et al. 2008) and direct evidence in the case of a few very extended GCs (see Jordi et al. 2009; Frank et al. 2012) and massive open clusters de Grijs & Parmentier 2007). The effect of initial mass segregation on low-mass depletion depends on the ratio between the onset of dissolution (due to tidal stripping) and the core collapse time. If dissolution starts before core collapse, mass segregation is still imprinted on the cluster and the low-mass depletion is severe. However, if core collapse occurs before the onset of dissolution, the effect of the initial mass segregation is erased and the low-mass depletion is about the same as in initially unsegregated clusters; see also (Baumgardt et al. 2008; Vesperini et al. 2009).

So, if open clusters start mass segregated, as suggested by observations, and are initially nearly Roche-volume filling, the low-mass depletion will start earlier than predicted by our models. In that case the MF may still be described by our analytic expressions of the DMF, but with larger values of $t_{depl}$ and $\Delta_{depl}$.

## 8 SUMMARY

We have studied the evolution of the global stellar MF of clusters, based on the results of a large grid of *N*-body simulations. These *N*-body simulations show that

(a) if the MF of different clusters are compared at the same age, $t$, or at the same dynamical age $t/t_{1\%}$ then the MF can be very different;

(b) if the MF are compared at the same residual mass fraction $M(t)/M_i$ then they show a strong similarity.

Based on this fact we showed that the evolution of the MF can be described by a simple set of analytical formula, if it is expressed in terms of the DMF $\Delta(\mu, m)$ with $\Delta = \log (N(m)/N_i(m))$, where $\mu = M(t)/M_i$ is the remaining mass fraction of the cluster. The function $\Delta$ depends on only two parameters: the depletion mass, which is the stellar mass where the slope of the MF starts to change, and $M_{lum}(t)/M_{lum}(t_{depl})$ which is the ratio between the present mass of the luminous (non-remnant) stars and the one at $t_{depl}$. We present expressions for estimating $M_{lum}(t)/M_{lum}(t_{depl})$ and $t_{depl}$. A comparison between the MFs derived by *N*-body simulations and predicted

by our formalism, shows very good agreement for clusters that have lost less than about 90 per cent of their initial mass.

Our method can be applied to predict the MF evolution of clusters in different environments and can be used to predict the photometric evolution and mass-luminosity ratios.[6] In a subsequent paper we will compare the predicted MFs of galactic GCs with observations.

In two appendices we provide formulae for the mass history $M(t)/M_i$ of clusters and for estimating the mass fraction of dark remnants in clusters as a function of time.

## REFERENCES

Alexander P. E. R., Gieles M., 2012, MNRAS, 422, 3415
Baumgardt H., Makino J., 2003, MNRAS, 340, 227
Baumgardt H., De Marchi G., Kroupa P., 2008, ApJ, 685, 247
Binney J., Tremaine S., 1987, Galactic Dynamics. Princeton Univ. Press, Princeton, NJ, p. 747
Chernoff D. F., Weinberg M. D., 1990, ApJ, 351, 121
de Grijs R., Parmentier G., 2007, Chin. J. Astron. Astrophys., 7, 155
Frank M. J., Hilker M., Baumgardt H., Côté P., Grebel E. K., Haghi H., Küpper A. H. W., Djorgovski S. G., 2012, MNRAS, 423, 2917
Gieles M., Portegies Zwart S. F., Baumgardt H., Athanassoula E., Lamers H. J. G. L. M., Sipior M., Leenaarts J., 2006, MNRAS, 371, 793
Gieles M., Athanassoula E., Portegies Zwart S. F., 2007, MNRAS, 376, 809
Gieles M., Baumgardt H., Heggie D. C., Lamers H. J. G. L. M., 2010, MNRAS, 408, L16
Gürkan M. A., Freitag M., Rasio F. A., 2004, ApJ, 604, 632
Hénon M., 1969, A&A, 2, 151
Hurley J. R., Pols O. R., Tout C. A., 2000, MNRAS, 315, 543
Jordi K. et al., 2009, AJ, 137, 4586
King I., 1958, AJ, 63, 114
King I. R., 1966, AJ, 71, 64
Kroupa P., 2001, MNRAS, 322, 231
Kruijssen J. M. D., 2009, A&A, 507, 1409
Lamers H. J. G. L. M., Gieles M., 2006, A&A, 455, L17
Lamers H. J. G. L. M., Gieles M., Bastian N., Baumgardt H., Kharchenko N. V., Portegies Zwart S., 2005, A&A, 441, 117
Lamers H. J. G. L. M., Baumgardt H., Gieles M., 2010, MNRAS, 409, 305
Portegies Zwart S. F., McMillan S. L. W., 2002, ApJ, 576, 899
Portegies Zwart S. F., McMillan S. L. W., Hut P., Makino J., 2001, MNRAS, 321, 199
Portegies Zwart S. F., McMillan S. L. W., Gieles M., 2010, ARA&A, 48, 431
Salpeter E. E., 1955, ApJ, 121, 161
Spitzer L. Jr, 1969, ApJ, 158, L139
Takahashi K., Portegies Zwart S. F., 2000, ApJ, 535, 759
Trenti M., Vesperini E., Pasquato M., 2010, ApJ, 708, 1598

---

[5] Hard binaries have a stronger effect on the cluster evolution because they heat the cluster. However, the fraction of initially formed hard binaries is expected to be small as most hard binaries form by three-body interactions.

[6] Our method will be used in the next generation of the EMACSS-program (Alexander & Gieles 2012) that describes the evolution of the cluster parameters for a wide range of initial properties and environments.

Vesperini E., 1997, MNRAS, 287, 915

Vesperini E., McMillan S. L. W., Portegies Zwart S., 2009, ApJ, 698, 615

## APPENDIX A: A SIMPLE METHOD TO PREDICT MASS EVOLUTION

The mass evolution, $M(t)$, depends on stellar evolution and the dynamical mass-loss (dissolution).

(a) The stellar evolutionary (se) mass-loss and the formation of remnants in clusters with different metallicities and different kick-fractions of black holes, neutron stars and white dwarfs can be calculated using the power-law approximations given in appendix B of LBG10. These equations can be used to calculate $\mu_{se}$ and $\mu_{se}^{rem}$ or their complements $q_{se} = 1 - \mu_{se}$ and $q_{se}^{rem} = 1 - \mu_{se}^{rem}$, as well as the mean mass of the luminous stars and the remnants in case of no dissolution.

(b) The dynamical mass-loss of a cluster can be described by $(dM/dt)_{dis} = -M/t_{dis} = -M^{1-\gamma}/t_0$ with $t_0$ described by LBG10 for clusters moving in a galaxy with a logarithmic potential, i.e. with a flat rotation curve, and by Gieles et al. (2006) and Gieles, Athanassoula & Portegies Zwart (2007) for clusters that experience shocks by spirals or by encounters with giant molecular clouds. LBG10 showed that the dissolution time-scale for clusters in a galaxy with a flat rotation curve and a Kroupa IMF is

$$t_0 = t_{ref}^{N} \left( \frac{<m>}{M_\odot} \right)^{-\gamma} \left( \frac{R_{gal}}{8.5\,kpc} \right) \left( \frac{220\,km/s}{v_{gal}} \right) (1 - \epsilon) \quad (A1)$$

with $t_{ref}^{N} = 13.3$ Myr and $\gamma = 0.65$ for clusters with an initial density profile with a King parameter of $W_0 = 5$ and $t_{ref}^{N} = 3.5$ Myr and $\gamma = 0.80$ if $W_0 = 7$. In this expression $R_{gal}$ and $\epsilon$ are respectively the apogalactic distance and eccentricity of the cluster orbit. The mean stellar mass before core collapse is $<m> \simeq 0.5 M_\odot$ for clusters with a Kroupa IMF.

(c) Following the method of Lamers et al. (2005), modified with the results of LBG10, we can describe the total mass evolution of the cluster

$$\mu(t) = M(t)/M_i = [\{1 - (1 + f_{ind}^{se}) q_{se}(t)\}^{\gamma} - (\gamma t/t_0) M_i^{-\gamma}]^{1/\gamma} \quad (A2)$$

if $t < t_{cc}$ and

$$\mu(t) = \mu_{cc} [\{1 - (1 + f_{ind}^{se})(q_{se}(t) - q_{se}(t_{cc}))\}^{\gamma_{cc}}$$
$$- (\gamma_{cc}(t - t_{cc})/t_0^{cc})(M_i \mu_{cc})^{-\gamma_{cc}}]^{1/\gamma_{cc}} \quad (A3)$$

if $t > t_{cc}$, where $t_{cc}$ is the core collapse time. This can be approximated by

$$t_{cc} \simeq 32 \times t_{rh0}^{0.872} \mathfrak{F}^{-0.51} \quad (A4)$$

where $\mathfrak{F} = \mathfrak{F}_5 = (r_h/r_J)/0.187$ if initial density distribution is a King model with $W_0 = 5$ and $\mathfrak{F} = \mathfrak{F}_7 = (r_h/r_J)/0.116$ if $W_0 = 7$ (LBG10).

In these expressions $\mu_{cc}$ is the fractional mass of the cluster at core collapse, which follows from equation (A2) at $t_{cc}$, and $\gamma_{cc} = 0.70$. The factor $f_{ind}^{se}$ describes the fraction of evolution-induced dynamical mass-loss. For initially Roche-volume UF models $f_{ind}^{se} = 0$. For initially Roche-volume filling clusters it is

$$f_{ind}^{se} \simeq 0.25 \, \log(t_0 M_i^{\gamma}/10^3) \times (1 - \epsilon)^3, \quad (A5)$$

when $t_0$ is in Myrs and $\epsilon$ is the eccentricity of the orbit. If tidal stripping is the dominant dissolution mechanism, then

$$t_0^{cc} = t_0 (\mu_{cc} M_i)^{\gamma - 0.70}/j_{cc} \quad (A6)$$
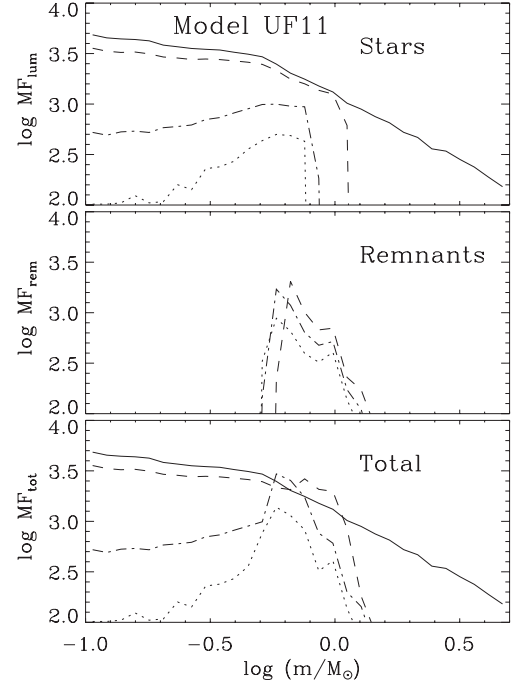


**Figure B1.** The MF in terms of number/bin of the luminous stars (top), remnants (centre) and total stars (bottom) of cluster model uf11. The bin-width is $\Delta \log m = 0.0567$. The model has a total lifetime of 20.8 Gyr. The MFs are shown at four times: when $\mu = 1.0$ (0 Gyr, full line), 0.5 (4.35 Gyr, dashed), 0.2 (13.0 Gyr, dash–dotted) and 0.1 (16.25 Gyr, dotted). As time progresses the lower mass limit of the white dwarfs decreases due to stellar evolution but the total number of remnants decreases due to dissolution.

and

$$j_{cc} \simeq -0.25 + 0.375 \times \log(t_0 M_i^{\gamma}). \quad (A7)$$

If shocks are the dominant dissolution mechanism, then $t_0^{cc} = t_0$, which is set by the strength and frequency of the shocks (Gieles et al. 2006, 2007; Lamers & Gieles 2006).

With this set of equations the mass history $\mu(t)$ can be calculated.[7]

## APPENDIX B: THE TOTAL MASS OF THE REMNANTS

The mass of the remnants in the clusters at any time depends on (a) the mass fraction of the remnants that are formed by stellar evolution and (b) the fraction of these remnants that are lost by dissolution.

Fig. B1 shows the evolution of the MF of the luminous stars and remnants of model uf11, that has a lifetime of $t_{1\%} = 20.8$ Gyr. At $t = 4.3$ Gyr ($\mu = 0.50$) the cluster contains white dwarfs and neutron stars with $0.56 < m < 1.34 M_\odot$. As time progresses and $\mu$ decreases the lower mass limit of the white dwarfs decreases, but the total number of neutron stars and white dwarfs also decreases because they are lost by dissolution.

In LBG10, we have provided simple power-law approximations that describe the formation rates of black holes, neutron stars and white dwarfs in clusters with a Kroupa IMF for different metallicities between $Z = 0.0004$ (1/50 solar) and 0.02 (solar). These are based on the evolution calculations of Hurley, Pols & Tout

---

[7] An IDL-program for the calculation of M(t) is available upon request from the first author.

(2000). Together with adopted kick-out fractions of these remnants this provides an accurate prediction for the mass fraction $\mu_{\rm rem}^{\rm se}(t) \equiv M_{\rm rem}/M_{\rm i}$ of remnants that are formed by stellar evolution with an accuracy better than a few per cent. Part of this fraction is subsequently lost by dissolution.

A study of all models with a Kroupa IMF between $0.1 < m/{\rm M}_\odot < 100$ with kick-out fractions of $f_{\rm kick}^{\rm bh} = f_{\rm kick}^{\rm ns} = 0.9$ and $f_{\rm kick}^{\rm wd} = 0$, i.e. models uf1 to uf16, shows that we can approximate

$$g_{\rm rem} \equiv \frac{\mu_{\rm rem}}{\mu_{\rm rem}^{\rm se}} = a \times \mu_{\rm dis} + b \times \mu_{\rm dis}^2 + (1 - a - b) \times \mu_{\rm dis}^3, \qquad (\text{B1})$$

where $\mu \equiv M/M_{\rm i}$ and $\mu_{\rm dis}$ is the mass fraction that the cluster would have if there was no stellar evolution,

$$\mu_{\rm dis} = \left[ 1 - \frac{\gamma t}{t_0} M_i^{-\gamma} \right]^{1/\gamma}. \qquad (\text{B2})$$

Expression (B1) is forced to have $g_{\rm rem} = 1$ at $\mu_{\rm dis} = 1$ and $g_{\rm rem} = 0$ at $\mu_{\rm dis} = 0$ because at $t \simeq 0$ or $\mu_{\rm dis} = 1$ the remnants are first formed before they are lost by dissolution (so $\mu_{\rm rem} = \mu_{\rm rem}^{\rm se}$) and at the end of the clusters lifetime, i.e. at $\mu_{\rm dis} = 0$, all remnants are lost. We found a very good fit if $a = 2.493$ and $b = -2.974$. So the total mass of the remnants at any time is

$$M_{\rm remn} \simeq M_{\rm i} \cdot \mu_{\rm rem}^{\rm se} \cdot g_{\rm rem}. \qquad (\text{B3})$$

This paper has been typeset from a TEX/LATEX file prepared by the author.